

## A Solid Propellant Microthruster with Metal Igniter

K. L. Zhang<sup>a, \*</sup>, S. K. Chou<sup>a</sup>, S. S. Ang<sup>b</sup>

<sup>a</sup> Department of Mechanical Engineering, National University of Singapore, Singapore 119260

<sup>b</sup> Department of Electrical Engineering, University of Arkansas, Fayetteville, AR 72701, USA

### Abstract

A new solid propellant microthruster design is proposed here as a potential micropropulsion system for microspacecraft. The new design provides the microthruster a high degree of flexibility, maneuverability and integration. Single microthruster and microthruster layer have been successfully fabricated using microfabrication technologies. The feasibility of the novel design has been investigated and proven by microcombustion experiment, thrust and impulse testing. The performance of the solid propellant microthruster with metal igniter is also compared with that of a solid propellant microthruster with wire igniter.

**Keywords:** Micropropulsion; Microthruster; Solid Propellant; Metal Igniter, Thrust, Impulse

### \* Corresponding author.

Zhang Kaili, Micro Systems Technology Initiative (MSTI), Department of Mechanical Engineering, National University of Singapore, Singapore 119260; Tel: (65) 68744619, Fax: (65) 67791459, E-mail address: [engp1562@nus.edu.sg](mailto:engp1562@nus.edu.sg).

### 1. Introduction

The application of MEMS technologies to space filed initiates the up to date microspacecraft. The motivations behind the development of microspacecraft are to increase launch rates, reduce mission risk, and increase mission flexibility by launching a cluster of microspacecrafts rather than a single large conventional spacecraft. Building microspacecraft necessitates the development of every subsystem so as to maintain the high degree onboard capability. Micropropulsion is an important subsystem that should be addressed. The micropropulsion system has many potential applications in microspacecraft, such as attitude control, drag compensation and orbit adjust.

In recent times, some kinds of micropropulsion systems are being investigated, such as bio/mono-propellant microthruster, cold/hot-gas microthruster, field emission microthruster, and pulsed plasma microthruster [1]-[3]. The solid propellant microthruster is a relatively new class of micropropulsion system. Its concept is based on the combustion of the energetic propellant stored in the micro-chamber. The solid propellant microthruster has many advantages, such as minimized system complexity, no moving parts, and very low propellant leakage possibility. Therefore, the solid propellant microthruster is being studied extensively [4]-[7]. Their main design concepts are based on the three-layer sandwich configurations, which normally contain

three parts, namely, a combustion chamber, a micronozzle, and an igniter. A different design from sandwich configuration is proposed by Zhang *et al.* [8]. This design has some advantages over the former designs, such as better bonding quality, higher fabrication efficiency, and more design flexibility. Nevertheless, this design uses a special wire as the igniter, which is not optimum for batch fabrication and high level integration. In this paper, a new design is proposed, which not only owns the advantages of the design in Ref. [8], but also is more suitable for batch fabrication and high level integration.

### 2. Design and Fabrication

The schematic of a proposed single microthruster is shown in Fig. 1. In the design, a metal igniter is deposited on a glass layer. A silicon wafer is fabricated to contain a chamber and a convergent-divergent nozzle. The glass layer and the silicon layer are bonded together to form a three-dimensional microthruster. The chamber is filled with the solid propellant. Once ignited, the resultant gas expands through the nozzle producing the desired thrust and impulse. A larger piece of glass layer is employed and connection is made to the end of the glass protruding out from the silicon part of the microthruster.

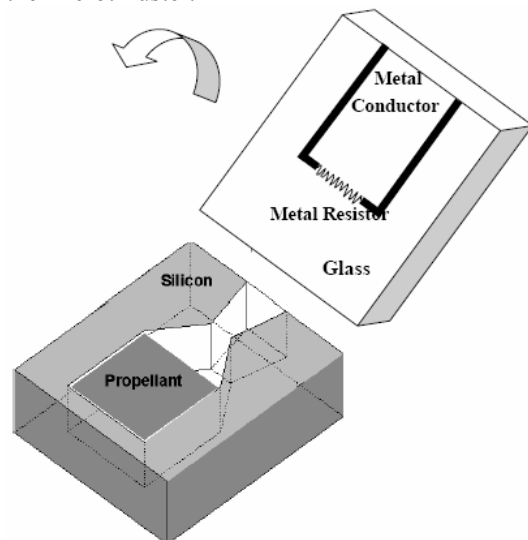


Fig. 1 Schematic of a single microthruster

The fabrication starts with a 550  $\mu\text{m}$  thick Pyrex-7740 glass substrate. Positive photo-resist is spin-coated onto the Pyrex glass and patterned using photolithography through a mask. A metal layer of Ti with the thickness of 206 nm is deposited by e-beam evaporation. Then a metal layer of Au with the thickness of 77 nm is deposited onto the Ti layer through e-beam evaporation. Metal Ti and Au lift-off

is performed in acetone with ultrasonic. The Pyrex substrate with Ti and Au metals is spin-coated and patterned using photo-lithography by a mask. After the exposed photoresist is removed, the substrate is put into Au etchant. The Au in the designed area is removed and the Ti is exposed as the resistor. The Pyrex substrate is diced into separate chips by a dicing machine. The SEM of the fabricated single igniter with Ti as the resistor and Au as the conductor is shown in Fig. 2.

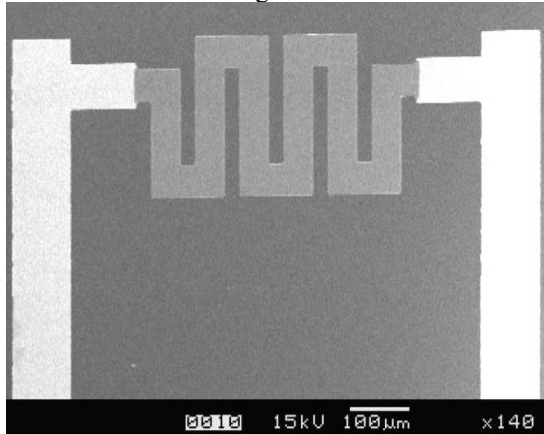


Fig. 2 SEM of Au/Ti igniter

A 750  $\mu\text{m}$  thick 4-inch (100) oriented silicon wafer is deposited by spin coating to a positive resist thickness of 12  $\mu\text{m}$ . After the resist is patterned by exposure to UV light through a mask, the exposed resist is developed. With the pattern transferred through photolithography, a deep reactive ion etching (DRIE) is performed on the silicon wafer. Then a thermal oxidation process is carried out. After thermal oxidation, the whole silicon wafer is covered by the silicon dioxide with a thickness of 246 nm. The resulting silicon wafer trench depth is 400  $\mu\text{m}$  after DRIE. The silicon wafer is diced into separate chips by a dicing machine. Figure 3 shows the front-side view of the microthruster. Figure 4 is the SEM of the microthruster cross-section. It can be seen that the sidewalls are vertical during and after the etching.

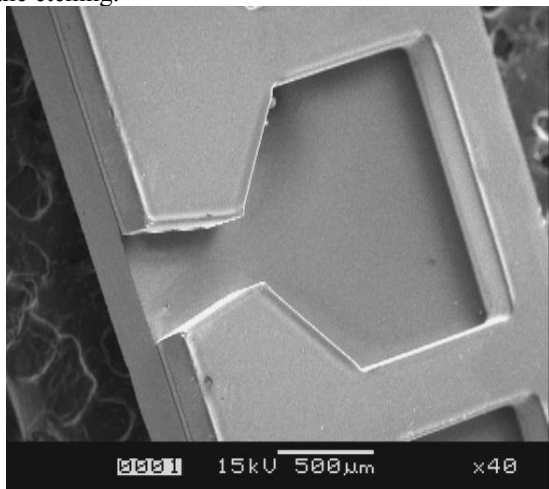


Fig. 3 SEM of the microthruster front-side

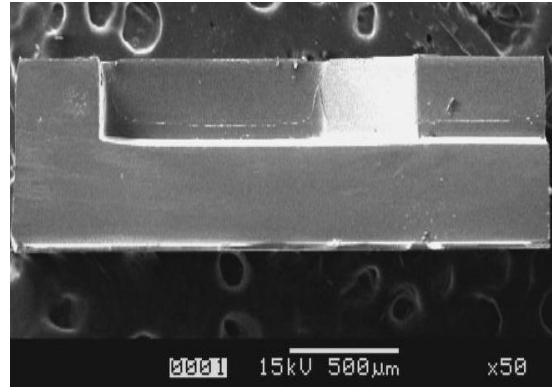


Fig. 4 SEM of the microthruster cross-section

The glass wafer with the Au/Ti igniter and the silicon wafer with the trench are bonded together by an anodic bonding process at 400  $^{\circ}\text{C}$  and a voltage of 1100 V. A reliable bond between the silicon layer and glass layer is then formed. The fabricated three-dimensional microthruster layer with igniter and solid propellant is shown in Fig. 5.

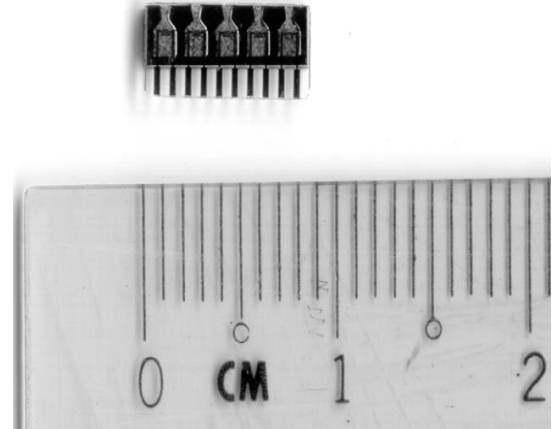


Fig. 5 3-D microthruster

The new design not only owns all the advantages of the design in Ref. [8], but also has several other advantages. Firstly, the new design employs the Au/Ti igniter instead of the wire igniter, which is more suitable for batch fabrication. Secondly, adding addressing capability is one key part of developing the microthruster array. The new design makes the realization of addressing capability easier. In addition, a higher level of integration can be possibly achieved. Lastly, the novel design makes it more convenient to observe the propellant combustion process visually inside the micro-scale device.

### 3. Experiment

A specific testing stand is developed to prove the feasibility of the design and to achieve the characteristics of the microthruster both at sea level and in vacuum. The stand consists of a high-speed digital video camera to capture the propellant combustion, a quartz piezoelectric force sensor with high sensitivity, a charge amplifier, a data acquisition system and a digital DC power supply to measure the thrust precisely. Detailed description of this part of the testing system can be found in Ref.

[8]. The characteristics of the microthruster in space are more important than those at sea level because the microspacecraft operate in space generally. Therefore, a vacuum system is combined into the testing system to simulate the performance of the microthruster in space as shown in Fig. 6.

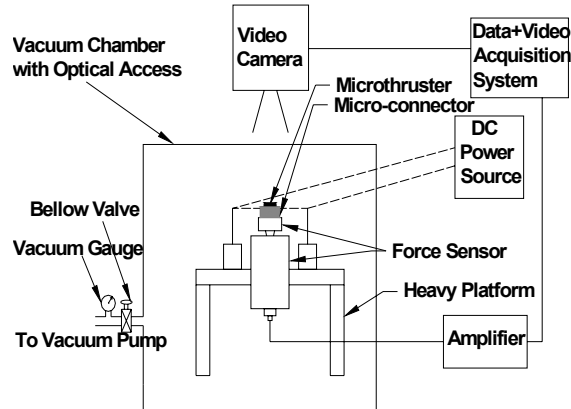


Fig. 6 Schematic of thrust testing system

### 3.1. Measurement Results

At the current experiment, the single solid propellant microthruster is firstly tested. The tested microthruster nozzle dimensions are: half divergence angle:  $12^\circ$ ; convergent length:  $500\ \mu\text{m}$ ; divergent length:  $600\ \mu\text{m}$ ; depth:  $400\ \mu\text{m}$ . The nozzle throat width is a variable. The chamber dimensions are  $1000 \times 1000 \times 400\ \mu\text{m}$  (length  $\times$  width  $\times$  depth). The  $100\ \mu\text{m}$  plane in the nozzle throat is to avoid sharp edges and facilitate the fabrication process.

Gunpowder-based solid propellant is employed here for the present experimental testing. The filled propellant mass has much effect on the microthruster performance in terms of specific impulse that is defined as the ratio of total impulse to propellant weight. Therefore, the propellant mass should be measured precisely before the firing. Table 1 shows the masses of the micro-thruster and propellant. The unfueled mass means the microthruster mass before loading, the fueled mass is the microthruster mass with the propellant loaded, and the mass fraction equals to the ratio of the propellant mass to the mass of the fueled microthruster before ignition.

Table 1 Mass of the microthruster and propellant

	Unfueled Mass (mg)	Fueled Mass (mg)	Propellant Mass (mg)	Mass Fraction (%)
Thruster	14.9	15.7	0.8	5.10

### 3.2. Microcombustion Experiment

Microcombustion experiment is performed to validate the feasibility visually of the solid propellant microthruster design. Continuous combustion is observed successfully after igniting the gunpowder-based solid propellant with the Au/Ti igniter. The combustion lasts for about 0.7 ms for a typical single microthruster. A series of frames from a high-speed digital video camera of the combustion are shown in

Fig. 7. A microthruster layer is installed into a micro-connector during the experiment. The images are acquired at 30,000 frames/s. The combustion process of the propellant can be visually observed in the novel design because of the transparent property of the Pyrex-7740 glass. It can be seen that the propellant is ignited initially at some point near the igniter. The combustion occurs and propagates to all the surface and then progresses rapidly. The ejected plume from the convergent-divergent nozzle exit can also be visually observed from Fig. 7.

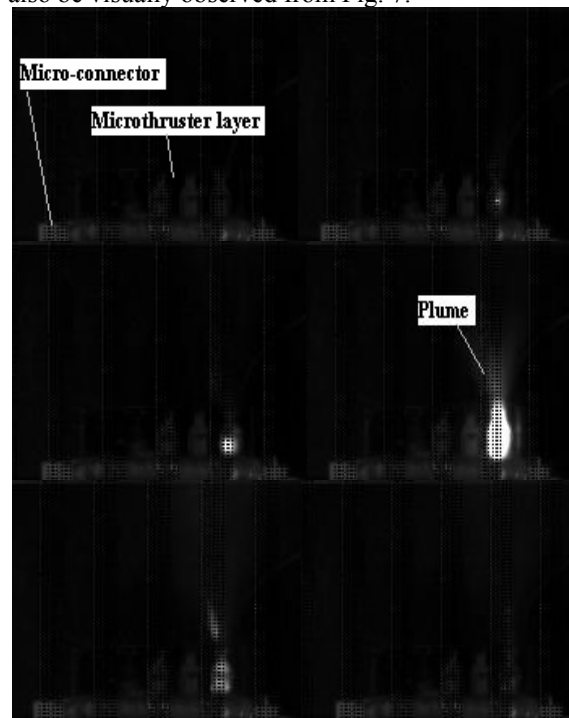


Fig. 7 Solid propellant microthruster firing (Images are acquired at 30,000 frames/s)

### 3.3. Thrust and Impulse Testing

The thrust and impulse measurements are performed both at sea level with the ambient temperature of approximately 300 K and in vacuum with the back pressure of 80 Pa. Figure 8 shows the performance at sea level and in vacuum for the microthruster with nozzle throat width of  $370\ \mu\text{m}$ . The peak thrust changes from 0.10 N to 0.43 N, the total impulse increases from  $3.28 \times 10^{-5}\ \text{N}\cdot\text{s}$  to  $1.44 \times 10^{-4}\ \text{N}\cdot\text{s}$ , and specific impulse increases from 4.18 s to 18.35 s when the back pressure changes from sea level to vacuum. The microthruster performance is considerably improved in vacuum. One reason for the improvement is the increase of the exit-ambient pressure difference in vacuum. The other possible reason is due to the flow pattern distinction of the microthruster jet. At sea level, the jet flow is probably subsonic because of the high back pressure. While in vacuum, the jet flow is probably supersonic due to the low back pressure. The supersonic jet produces higher thrust and impulse than the subsonic jet.

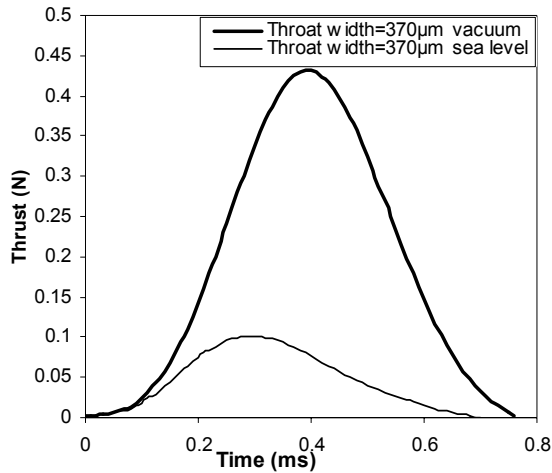


Fig. 8 Microthruster performance at sea level and in vacuum

### 3.4. Comparison between Microthrusters with Metal Igniter and Wire Igniter

A solid propellant microthruster with wire igniter is developed in Ref. [8], which has the similar design as the solid propellant microthruster with metal igniter. Figure 9 shows the performance comparison between the microthruster with Au/Ti igniter and the microthruster with wire igniter at sea level. The two kinds of microthrusters have same dimensions. The thrusts and total impulses produced by the microthrusters with Au/Ti igniter and wire igniter are similar. This is due to the same dimensions. Specific impulse produced by the microthruster with Au/Ti igniter is higher than that generated by the microthruster with wire igniter (14.65 s vs. 11.32 s), which is because of the lower propellant mass (Table 1) of the microthruster with Au/Ti igniter compared with that of the microthruster with wire igniter.

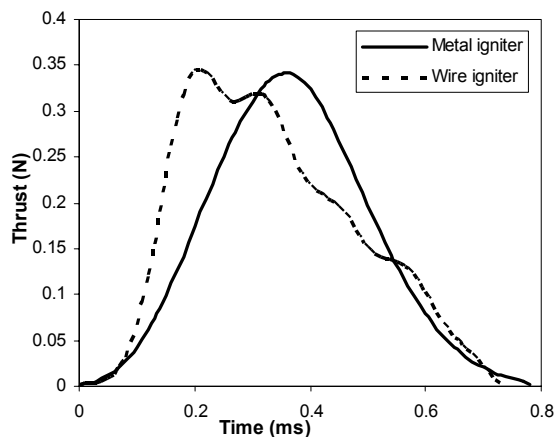


Fig. 9 Performance comparison between microthrusters with metal igniter and wire igniter

## 4. Conclusion

A novel MEMS solid propellant microthruster with metal igniter is developed. The new design is suitable for batch fabrication and high degree miniaturization. It has high fabrication efficiency,

much design flexibility and good bonding quality. The feasibility of the new design is proven by micro-combustion experiment, thrust and impulse measurements. The solid propellant microthruster with metal igniter presents similar total impulse, but higher specific impulse than the solid propellant microthruster with wire igniter.

## Acknowledgements

This work is funded by NUS under Grant R-265-000-150-112. The authors wish to acknowledge the support of the Institute of Materials Research and Engineering, NUS Micro System Technology Lab, Advanced Manufacture Lab, Impact Mechanics Lab, and Thermo Lab for their contributions to the propellant preparation, the microthruster fabrication and testing.

## References

- [1] J. Mueller, "Thruster Options for Micro-spacecraft: A Review and Evaluation of Existing Hardware and Emerging Technologies," in 33rd AIAA/ASME/SAE/ASEE Joint Propulsion Conf and Exhibit, 1997, AIAA Paper 97-3058.
- [2] E. Y. Choueiri, "Overview of U. S. Academic Programs in Electric Propulsion," in 35th AIAA Joint Propulsion Conference, 1999, AIAA Paper 99-2163.
- [3] A. P. London, A. H. Epstein, and J. L. Kerrebrock, "High-Pressure Bipropellant Micro-rocket Engine," *Journal of Propulsion and Power*, vol. 17, no. 4, 2001, pp. 780-787.
- [4] David H. Lewis Jr., Siegfried W. Janson, Ronald B. Cohen, and Erik K. Antonsson, "Digital Micro-propulsion," *Sensors and Actuators A*, vol. 80, 2000, pp. 143-154.
- [5] Daniel W. Youngner *et al*, "MEMS Mega-pixel Micro-thruster Arrays for Small Satellite Station-keeping," 14th Annual AIAA/USU Conference on Small Satellites, AIAA Paper SSC00-X-2, August 21-24, 2000.
- [6] Dana Teasdale, Veljko Milanovic, Paul Chang, and Kristofer S J Pister, "Microrockets for Smart Dust," *Smart Mater. Struct.*, vol. 10, 2001, pp. 1145-1155.
- [7] C. Rossi, S. Orioux, B. Larangot, T. Do Conto, and D. Esteve, "Design, Fabrication and Modeling of Solid Propellant Microrocket-Application to Micro-propulsion," *Sensors and Actuators A*, vol. 3280, 2002, pp. 1-9.
- [8] K. L. Zhang, S. K. Chou, and Simon S. Ang, "Development of a Solid Propellant Microthruster with Chamber and Nozzle Etched on a Wafer Surface," *Journal of Micromechanics and Micro-engineering*, vol. 14, no. 6, pp. 785-792, 2004.